PROCEEDINGS OF THE 15TH SYMPOSIUM ON THE GEOLOGY OF THE BAHAMAS AND OTHER CARBONATE REGIONS

Edited by
Douglas W. Gamble and Pascal Kindler

Gerace Research Center
San Salvador, Bahamas
2012

Front Cover: *Porites* colony encrusted by red algae in waters of San Salvador, Bahamas; see paper by Fowler and Griffing., p. 41. Photograph by Pascal Kindler, 2011.

Back Cover:. Dr. Jörn Geister, Naturhistorisches Museum Bern, Keynote Speaker for the 15th Symposium and author of "Keynote Address – Time-Traveling in a Caribbean Coral Reef (San Andres Island, Western Caribbean, Colombia)", this volume , p. vii. Photograph by Joan Mylroie.

Press: A & A Printing

ISBN 978-0-935909-93-7

NEW U/Th AND AMINO-ACID RACEMIZATION DATING AND INTERPRETATION OF PLEISTOCENE SEQUENCES FROM WEST CAICOS ISLAND (CAICOS PLATFORM): IMPLICATIONS FOR CYCLOSTRATIGRAPHY

Pascal Kindler and Aurélien Meyer
Section of Earth and Environmental Sciences
University of Geneva
1205 Geneva, Switzerland

ABSTRACT

The Pleistocene sequences covering West Caicos Island (Caicos Platform) show a more complicated geometry than previously thought and provide a good example of lateral and chronological variability of sediments deposited during the same sea-level history. Studied core transects at Boat Cove and Company Point on the western coast of the island display several vertically stacked, shallowing-upward sedimentary sequences comprising peri-reefal and/or oolitic facies, separated by soil zones. Previous interpretations proposed that these sequences were formed during distinct and successive interglacial sea-level highstands of the Pleistocene, whereas pedogenic horizons were correlated with glacial lowstands. Our new geochronological data show that the uppermost two sequences observed at the studied locations were both deposited during the last interglacial period, suggesting an intricate sea-level history during this time interval. In addition, the underlying sequence at Boat Cove must not be correlated with the penultimate interglacial highstand, but with an older highstand event in the middle Pleistocene. This example of lateral and temporal variability of meter-scale sequences must be remembered when applying cyclostratigraphic concepts to older carbonate successions.

INTRODUCTION

West Caicos is a low-elevation, NNE-SSW trending island located along the western margin of the Caicos Platform (SE Bahama Archipelago; Figure 1). About 10 km long and 3 km wide, it is mostly composed of Pleistocene deposits (Lloyd et al., 1987; Wanless and Dravis, 1989, 2008), including prominent eolianites that are subparallel to the axis of the island and form an older central spine of ridges with maximum elevations between 15 and 23 m (Figure 2). Large-scale cross bedding in these oolitic/peloidal grainstone ridges indicates a sediment source to the east. Wanless and Dravis (1989, 2008) and Dravis and Wanless (2008) hypothesized that these high ridges obstructed off-bank sediment transport for some time, thus permitting the growth of an upper Pleistocene reef in their lee, which now forms most of the rocky western coast of the island (Figure 2).

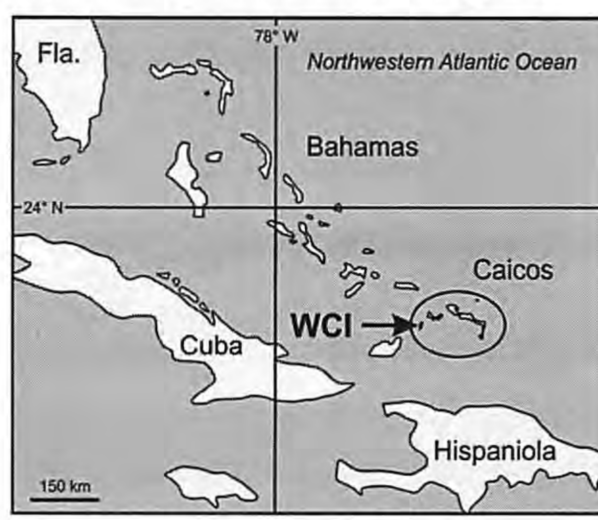

Figure 1. Location of study area. Fla. = Florida; WCI = West Caicos Island.

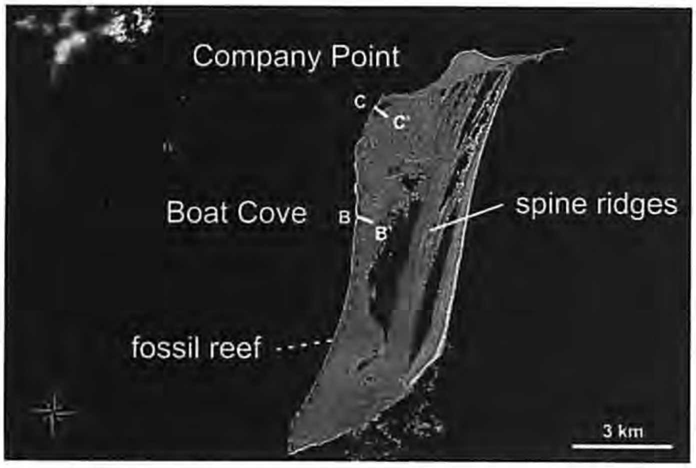

Figure 2. Satellite view of West Caicos Island showing the location of the core transects (B-B' and C-C'), the fossil reef (dashed line), and the central ridges mentioned in the text. Background photo from Google Earth.

In June 1985, H.R. Wanless and a group of students drilled two core transects across the NW corner of West Caicos (Figure 2). The system used to drill cores consisted of a light, hydraulic-driven rotary drill using NX bits, providing 1.25 inch (3.18 cm) diameter cores. In total, they worked on 12 sites, with coring depths of 15 m or less. The first transect was located near Company Point, to the NW of the northern end of the high ridges forming the backbone of West Caicos (Figure 2). This NW-SE trending transect was about 130 m long and comprised eight core borings. From NW to SE, it crossed Holocene beach-dune ridges, an active salina, and Pleistocene ridges. As shown by Waltz (1988) and Wanless and Dravis (1989, 2008), the most seaward core (# 6) comprised two vertically stacked Pleistocene oolitic-grainstone sequences covering weathered skeletal grainstone and overlain by Holocene sands; boreholes (# 1-4 and 7 from west to east) were similar, but their upper portion encompassed a Holocene evaporitic succession; the most landward core (# 8) penetrated only the Pleistocene record. The second transect, comprising four core borings, was located close to Boat Cove, on the protected western coast of the island (Figure 2). It was drilled near the northern termination of the Pleistocene reef and perpendicular to its axis to about 600 m inland. According to Waltz (1988) and Wanless and Dravis (1989, 2008), the three seaward cores (# 10, 9 and 11) mostly revealed one shallowing-upward sequence consisting of reefal material, whereas the most landward core (# 12), located about 500 m behind the reef, was drilled in backreef sediments and showed two vertically stacked reef to oolite sequences, separated by an exposure surface at a depth of about 8 m, and capping weathered skeletal grainstone.

Thanks to H.R. Wanless and J.J. Dravis, one of us (PK) had the opportunity to examine and re-sample cores # 4 and 12 in 2008. A total of 20 coral and whole-rock samples were collected for geochronological and geochemical analyses to obtain ages from the sequences described from the subsurface of West Caicos.

METHODS

Two main techniques were employed: uranium series and amino-acid racemization dating. We provide below a short summary of these methods; more complete information can be found in Hearty and Kaufmann (2000) and Edwards et al. (2003).

Uranium-series dating on corals

U-series measurements were performed at the Leibniz Intitute for Marine Sciences (IFM-GEOMAR) in Kiel, Germany. Element separation procedure follows previously published methods but used Eichrom-UTEVA resin (Fietzke et al., 2005). Determination of U- and Th-isotope ratios followed a multi-static, multi-ion-counting (MIC) ICP-MS approach (Fietzke et al., 2005). For isotope dilution measurements, a combined $^{233}U/^{236}U/^{229}Th$-spike was used, with stock solutions calibrated for concentration using NIST-SRM3164 (U) and NIST-SRM 3159 (Th) and, as combi-spike, calibrated against CRM-145 uranium standard solution (also known as NBL-112A) for U-isotope composition, and against a secular equilibrium standard (HU-1, uranium ore solution) for the precise determination of $^{230}Th/^{234}U$ activity ratios. Whole procedure blank values of this sample set were measured to be ~2 pg for Th and between 4 and 8 pg for U. Both values are in the typical range of this method and the laboratory. Ages were calculated using the equation of Fietzke et al. (2005). Samples are corrected for blanks and inherited ^{230}Th associated with detrital ^{230}Th assuming that the $^{230}Th/^{232}Th$ activity ratio is 0.6±0.2.

In the present research, the $^{230}Th/^{234}U$ method was specifically applied on corals because these organisms precipitate aragonite skeletons containing fair amounts of uranium (generally 2-3 ppm), but no thorium. After the death of the polyp, coral skeletons commonly behave as a closed geochemical system until the aragonite is dissolved or changes to calcite (James 1974). However, various early diagenetic processes (e.g. cementation, recrystallisation; Fruijtier et al., 2000; Kindler et al., 2007) can result in loss of uranium relative to thorium and produce erroneous ages. Thus, age measurements must only be performed on unaltered corals, which can be checked by thin-section examination and XRD analysis. The error margins on last-interglacial ages have now been narrowed down to less than 1000 years (Edwards et al., 2003), implying that this method can be used to reconstruct high-frequency sea-level fluctuations during this time period (Thompson and Goldstein, 2005).

Amino-acid racemization dating

Amino-acid racemization analyses were performed at the Amino Acid Geochronology Laboratory at Northern Arizona University. Alloisoleucine/isoleucine (or A/I) ratios were measured on whole-rock samples using ion-exchange chromatography and following a previously published methodology (Hearty and Kaufmann, 2000; 2009). Racemization is a time- and temperature-dependant diagenetic process consisting in the change of L-isomers of individual amino acids to the D-configuration. During amino-acid racemization (AAR), the L-enantiomers, which are present in living bodies, are converted to the corresponding D-enantiomers, and the reaction continues until it reaches an equilibrium state called a racemic mixture (Brown, 1985). In the Bahamas, Hearty and Kaufman (2009) estimated that equilibrium, with D/L ratio = 1.3, is achieved after >1 Ma, but D/L values >1.0 are rarely recorded as most exposed Bahamian rocks are younger than 0.5 Ma.

An AAR ratio does not give an age by itself. It is attributed to a specific aminozone that is calibrated with other dating techniques (^{14}C, U dating; Hearty and Kaufman, 2009). Based on data from Hearty and Kaufman (2000, 2009), Table 1 provides a list of the aminozones identified so far in the Bahamas region and indicates the time intervals to which they correspond.

This technique appears to offer an interesting potential as a mean of establishing relative chronology. In addition to shells, the use of whole-rock samples is becoming more and more important. Mitterer (1968) showed that coated grains contain concentrations of amino acids similar to those of mollusks. The whole-rock method has since been successfully applied mostly on Bermuda and the Bahamas (Hearty et al., 1992, Hearty and Kaufman, 2000, 2009). However, the technique has certain limitations, and datings must be used with a care. At present, several authors consider that it should not be used alone (Carew and Mylroie, 1995; Kindler et al., 2010), but in combination with other absolute and relative dating methods. Furthermore, amino-acid reactions are temperature dependent and, therefore, data can only be compared from areas that have the same climatic characteristics and thermal histories. In addition, the exact stratigraphic position of the samples has to be considered, as sediments lying close to the surface are exposed to greater seasonal temperature variations, and may then give anomalously high ratios. Moreover, pH (acidity/alkalinity) and water concentrations in the environment also influence the racemization rate of amino acids (Brown, 1985).

Table 1. Extent of isoleucine epimerization from whole-rock samples for various Bahamas islands. Each A/I ratio presented here corresponds to an average of up to 20 values obtained by Hearty and Kaufman (2000) per lithostratigraphic unit and per island. APK calibrated age have been calculated accorded to the formula proposed by Hearty and Kaufman (2000). Duration of Marine Isotope Stages are based on Siddall et al. (2010) for MIS 1 to 7, and on Bassinot et al. (1997) for MIS 9 to >13. Islands are listed according to their latitude (northernmost island at the top of the list) which emphasizes the slight increase in A/I ratios towards the south, corresponding to the temperature trend. Stratigraphic nomenclature is based on the review made by Kindler et al. (2010): HBM = Hanna Bay Member; NPM = North Point Member; WPM = Whale Point Member; CTM = Cockburn Town Member; FBM = French Bay Member; OHF 1 to 3 = members of the Owl's Hole Formation.

	BAHAMIAN LITHOSTRATIGRAPHIC UNITS							
	HBM	NPM	WPM	CTM	FBM	OHF3	OHF2	OHF1
ISLANDS								
Grand Bahama				0.36	0.41	0.47		
Abaco		0.12	0.28	0.36		0.54	0.64	
Andros	0.04			0.37	0.47		0.69	
New Providence		0.09	0.27	0.36		0.56	0.69	
Eleuthera		0.11	0.29	0.38		0.58	0.66	
Cat		0.12		0.37		0.57	0.65	0.76
Exuma	0.04	0.10	0.34	0.40	0.49	0.59	0.67	
San Salvador	0.09	0.15	0.33	0.40	0.50		0.69	
Long		0.10	0.32	0.43		0.55		0.87
Acklins		0.10		0.44		0.57		
Mayaguana	0.06			0.45				0.93
Caicos	0.08			0.42				
Inagua	0.05			0.48			0.77	
	0.09			0.43				
average	0.06	0.11	0.31	0.40	0.47	0.55	0.68	0.85
AMINOZONES	A		C	E		F/G	H	I
Marine Isotope Stage	1		5a	5e		7/9	11	>13
MIS duration (ka BP)	0 - 7		77.5 - 85	116 - 124		186 - 328	364 -406	> 524
APK calibrated age (ka BP)	6.27		86.8	125		281.2	432.9	680.5

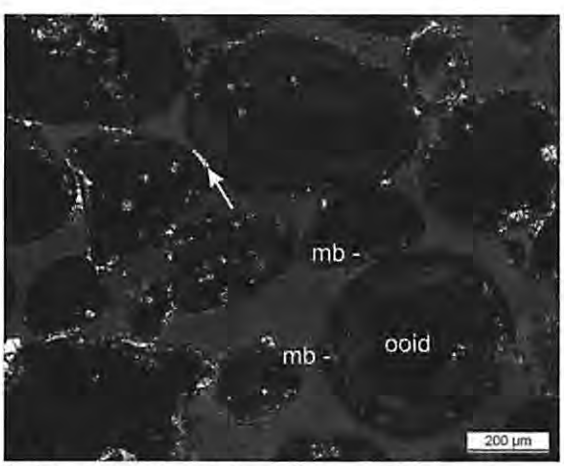

Figure 3. Sample CC1, core # 12, 2.0 mbs. Microfacies of Unit 1 : poorly cemented oolitic-peloidal grainstone. Note rare low-Mg calcite meniscus cement (white arrow), partial micritization of ooids, and numerous microborings (mb) of probable algal origin.

RESULTS

Boat Cove

In this study, we thoroughly examined the lithologies found in core # 12 which is approximately 11 m long. Recovery was excellent in the bottom half of the core, but poor for the upper half, preventing a precise estimate of the depth for the first samples. We identified five lithologic units of distinctive petrographic composition.

Unit 1 (sections 1 to 6; 0 to 6 mbs = meters below the surface). This unit is mostly composed of laminated oolitic-peloidal grainstone with mm-sized bioclasts (mainly *Halimeda* and mollusk fragments. Ooids are often partly micritized and display numerous algal microborings (Figure 3). Grains are bound by low-Mg calcite (LMC) crystals forming menisci at grain contacts. Because some laminae underwent more diagenesis than others, porosity and permeability vary laterally and vertically. Coral-rich horizons have been observed in the lower part of this unit (Wanless and Dravis, 1989), but no samples from these layers could be recovered for this study. One oolite sample collected at 2.0 mbs yielded an A/I ratio of 0.406±0.002, corresponding to aminozone E1 of Hearty and Kaufman (2009).

Unit 2 (sections 7 to 9; 6 to 7.8 mbs). The upper part of this unit consists of fine-grained oolitic-peloidal grainstone with scattered mm-sized bioclasts, very similar to the main lithology found in Unit 1. Sample CC2 collected near the top of Unit 2, just below 6 mbs, further shows superimposed pedogenic features such as needle-fiber calcite, root-hair sheaths, and micritized zones. The lower part of this unit contains numerous fragments of massive corals (*Montastraea annularis*, *Diploria labyrinthiformis*) and large *Strombus* gastropod shells. In thin section, coral skeletons exhibit dense fibrous aragonite with rare fungal borings, however XRD analyses indicate that collected samples contain up to 10% of calcite. Sample CC2 gave an A/I ratio of 0.402±0.005, corresponding to aminozone E1 of Hearty and Kaufman (2009), whereas coral specimens from the top and the base of the coral-rich interval gave ages of 120.85±0.80 ka and 131.05±1.32 ka, respectively (Table 2).

Unit 3 (sections 10 to 12; 7.8 to 8.7 mbs). This unit is made of partly leached and recrystallized oolitic-peloidal grainstone/ floatstone with bioclasts (Figure 4), mainly *Halimeda* and bivalve fragments. LMC cement is much more widespread than in the upper two units and occurs as drusy fillings and as menisci at grain contacts. One sample collected from this portion (CC6 at 8.4 m) further displays micritic crusts, needle-fiber calcite and root cells indicative of pedogenesis. Samples gathered from the top and the base of this unit gave A/I ratios of 0.710±0.016 and 0.669±0.008, respectively, correlating with aminozone H of Hearty and Kaufman (2009).

Unit 4 (sections 13 and 14; 8.7 to 9.5 mbs). The unit consists of well-lithified coral framestone or rudstone (the difference is hard to distinguish in core studies) with an oolitic grainstone matrix (Figure 5). Cm-sized coral branches (or clasts) are encrusted by a variety of organisms including red algae, foraminifers, and serpulids. The occurrence of needle-fiber calcite and pervasive leaching and micritisation indicate these rocks have undergone pedogenic alteration. One sample from the base of this unit yielded an A/I ratio of 0.692±0.009, corresponding to aminozone H of Hearty and Kaufman (2009).

Unit 5 (sections 15 to 17; 9.5 to 11 mbs). This unit shows a rudstone texture. Cm-sized clasts consisting of coarse bioclastic grainstone with recrystallized *Halimeda* and mollusk fragments are linked by micritic bridges forming an alveolar septal structure (Figure 6). The grainstone clasts show an early generation of recrystallized isopachous fibrous cement and a late phase of LMC sparry cement filling the remaining pore spaces. Samples collected from the top and base of this unit gave A/I ratios of

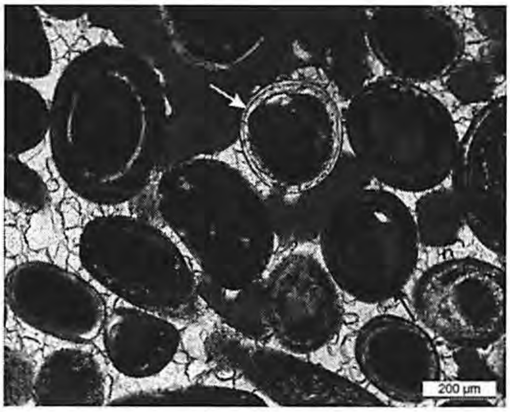

Figure 4. Sample CC5, core # 12, 8.0 mbs. Microfacies of Unit 3 : well-cemented oolitic-peloidal grainstone. Note leached (black arrow) and calcitized (white arrow) ooids. Rock composition is similar to that of sample CC1 (Figure 3), but diagenetic alteration is more advanced due to greater age.

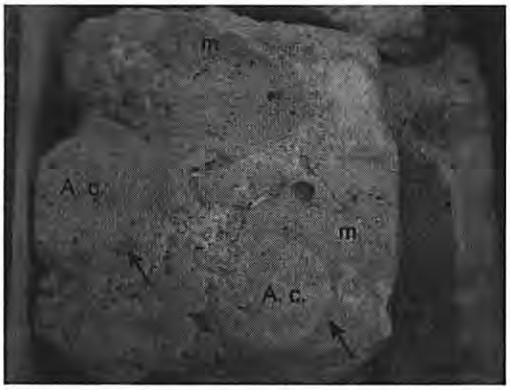

Figure 5. Sample CC8, core # 12, 9.0 mbs. Macrofacies of Unit 4 : well-lithified coral framestone/rudstone. A. c. = Acropora cervicornis branches; m = oolitic packstone matrix; arrows point to red-algal crust around coral branches.

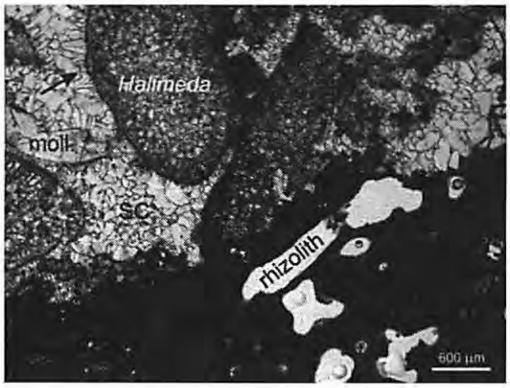

Figure 6. Sample CC12, core # 12, 10.8 mbs. Microfacies of Unit 5 : well-cemented bioclastic grainstone showing an early generation of isopachous fibrous cement (black arrow) and a late phase of LMC sparry cement (SC). Lower part of photo corresponds to a pedogenically altered zone. This grainstone has been brecciated by root activity.

0.513±0.016 and 0.432±0.020, respectively. The latter value measured on a low-concentration residue must be discarded, and the former can be correlated with aminozone F/G of Hearty and Kaufman (2009).

Company Point

Core # 4 is approximately 11 m long. We have focused on the Pleistocene record of this core which is found between ~2.5 and 11 mbs and comprises three lithologic units.

Unit A (sections 1 and 2 p.p.; 2.5 to 4 mbs). It is made of poorly lithified oolitic-peloidal grainstone with rare *Halimeda* fragments. The upper part of the unit is finely laminated, with fine-grained laminae being more cemented than coarse-grained layers (Figure 7), whereas the lower part shows a mottled texture indicative of bioturbation. Two samples collected from the laminated part of Unit A gave A/I ratios of 0.389±0.008 and 0.398±0.009, correlating with aminozone E1 of Hearty and Kaufman (2009).

Unit B (sections 2 p.p. to 5; 4 to 10 mbs). This unit consists of poorly lithified bioclastic floatstone with a fine-grained oolitic matrix (Figure 8). Larger grains include bioclasts (*Halimeda* and mollusk fragments), aggregates and oolitic grainstone lithoclasts. LMC cement is patchy. It can be finely crystalline, filling pore spaces and forming menisci at grain contacts, or, surprisingly, comprise large crystals that engulf constituent grains (poikilotopic cement, Figure 8; Flügel, 2004). The upper part of the unit is crudely laminated, whereas the lower part shows a mottled structure indicative of bioturbation. Samples collected from this unit yielded A/I ratios of 0.421±0.006 and 0.384±0.000, correlating with aminozone E1 of Hearty and Kaufman (2009).

Unit C (section 6; 10 to 11 mbs). This unit is composed of coral framestone/rudstone with a bioclastic grainstone/boundstone matrix. Important micritization in the upper part of the unit suggests that it has been exposed to pedogenic processes. In the lower part of the unit, the matrix grains are bound by micritic filaments of biogenic (? microbial) origin (Figure 9; Hillgärtner et al., 2001), and must thus be described as a boundstone. One sample collected from this unit gave an A/I ratio of 0.479±0.005, corresponding with aminozone F/G of Hearty and Kaufman (2009).

Table 2. U-Th data from core # 12, Boat Cove, West Caicos Island

Sample	Sec.*	Co.†	Calcite	Height	Age	±	^{238}U	±	^{232}Th	±	δ^{234}U(0)§	±	δ^{234}U(T)#	±	Rel.**
			(%)	(mbs)	kyr	kyr	ppm	ppm	ppb	ppb	‰	‰	‰	‰	
CC 3	7	Ma	9.9	6.0	**120.85**	**0.80**	2.244	0.002	6.24	0.05	99	2	138	2	mr
CC 4	9	Dl	6.9	7.0	**131.05**	**1.32**	2.598	0.003	39.06	0.12	96	2	139	2	mr

Note: Samples are stored at the Department of Geology, CH-1205 Geneva, Switzerland.

*Number of the core section where sample was collected.

†Co. = coral species: Dl = *Diploria labyrinthiformis*; Ma = *Montastrea annularis*.

§measured ^{234}U/^{238}U activity ratios (δ^{234}U(0)) are presented as deviation per mil (‰) from the equilibrium value.

#decay corrected ^{234}U/^{238}U activity ratios (δ^{234}U(T)) are calculated from the given ages and with λ_{234U}: 2.8263x10^{-6} yr^{-1}.

**Rel. = reliability: ages are strictly reliable (sr) having pristine δ^{234}U(T) values between 146.6 and 149.6 ‰; reliable (r) with values of 149.6±8 ‰ reflecting ages within 2 kyr of the true age; moderately reliable (mr) in other cases.

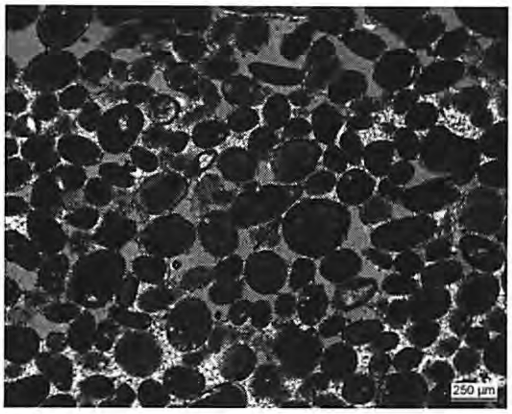

Figure 7. Sample CC16, core # 4, 3.0 mbs. Microfacies of the upper part of Unit A : finely laminated oolitic-peloidal grainstone. Fine-grained laminae are well cemented, whereas only LMC menisci (black arrow) occur in coarse-grained laminae. Such fine lamination commonly characterizes eolian deposits (e.g. Caputo, 1995).

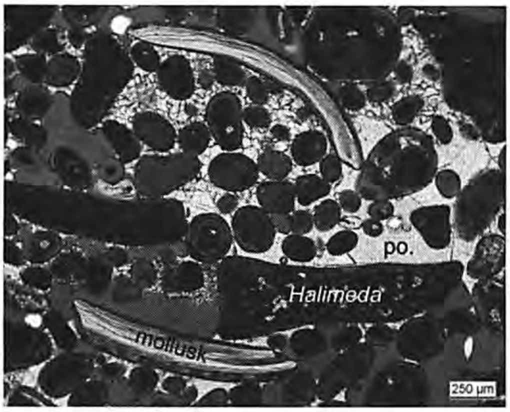

Figure 8 . Sample CC18, core # 4, 8.0 mbs. Microfacies of the lower, bioturbated part of Unit B : bioclastic floatstone with an oolitic-peloidal matrix. Except for the numerous bioclasts, the lithology is very similar to that of Unit A (Figure 7). Note patchy LMC cement filling pore spaces, forming menisci at grain contacts, and locally engulfing several grains (po. = poikilotopic cement).

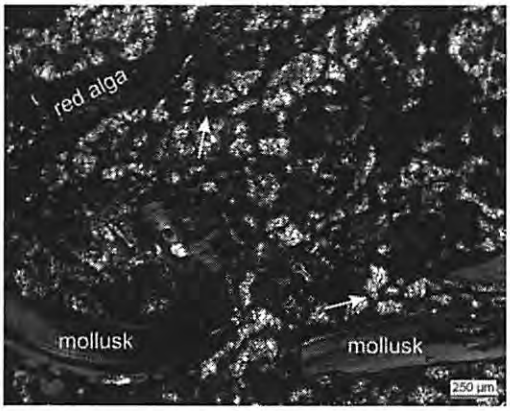

Figure 9. Sample CC20, core # 4, 10.8 mbs. Microfacies of Unit C : bioclastic boundstone. Note that constituent grains (mollusk, foraminifers, coral) have been bound by micritic filaments of microbial origin (white arrows).

DISCUSSION

Past depositional settings

Inferring past depositional environments from core borings is a difficult task because the large-scale geometry of drilled rock bodies is missing. Furthermore, as mentioned above, various rock types, such as framestone and rudstone are not easily distinguishable in core samples. Nonetheless, based on previous literature (Wanless and Dravis, 1989, 2008; Dravis and Wanless, 2008), core re-examination, and field observations made by one of us (PK) in West Caicos, the following interpretations can be proposed.

Units 1, 2, and 3+4 identified in core # 12 at Boat Cove correspond to three vertically stacked reef to oolite sequences (Walz, 1988; Wanless and Dravis, 1989), which form when a reef is buried by contemporaneous oolitic sands. Examples dating from the late Pleistocene can be observed at several locations along the western coast of West Caicos (Figure 10) and can be seen forming along the NW corner of the island today. We interpret the underlying Unit 5 as diagenetic rudstone resulting from the brecciation of a bioclastic grainstone by root activity in a soil zone. The occurrence of an early phase of isopachous fibrous cement in this grainstone suggests that diagenesis first occurred in a phreatic marine setting, and leads us to consider these rocks as remnants of a submarine hardground.

As proposed by Wanless and Dravis (1989), Units A and B found in core # 4 at Company Point represent two vertically stacked shallowing-upward sequences of burrowed and laminated oolite, corresponding to deep- and shallow-subtidal environments, respectively. Pleistocene examples of such sequences can be observed near Boat Cove, and modern equivalents can be seen (and sampled) at Ambergris Cay ooid shoal (Rankey et al., 2008). Finally, the skeletal limestone (framestone, rudstone and boundstone) composing Unit C in core # 4 was probably deposited in a peri-reefal setting.

Sequence ages

The upper reef to oolite sequences in core # 12 (Boat Cove, Units 1 and 2) can both be correlated with the last interglacial period, Marine Isotope Stage 5e, as indicated by two U-Th dates in stratigraphic order (~130 and 120 ka; Table 2; Figure 11) and A/I ratios associated with aminozone E1 (Table 1; Hearty and Kaufman, 2009). This relatively young age is supported by the minor diagenetic alteration of these two sequences (Figure 3). The lower reef to oolite sequence (Units 3+4) can be attributed to MIS 11, based on three A/I ratios ranging between 0.669 and 0.710, and thus constrained to aminozone H (Table 1; Hearty and Kaufman, 2009). The apparent stratigraphic inversion noted in this sequence could be due either to a temperature effect, that elevated the A/I ratio of the upper sample, or to a mixing of core fragments in the core box. The older age of this sequence is corroborated by a higher degree of diagenetic alteration (leached and calcitized ooids; Figure 4) compared to the overlying sequences. The basal diagenetic rudstone (Unit 5) in core # 12 gave one single A/I ratio of 0.513, correlating with aminozone F (Table 1; Hearty and Kaufman, 2009), i.e. the penultimate interglacial period (MIS 7). The elementary stratigraphic principle of superposition clearly shows that this result is flawed. The obtained value could result from pedogenic alteration or, alternatively, indicate that Unit 5 dates from the early Pleistocene, when the pattern of increasing A/I ratios with greater age reverses due to low amino-acid concentrations in analyzed samples (Hearty, 2010).

Both shallowing-upward oolitic sequences in core # 4 (Company Point; Units A and B) can be correlated with MIS 5e, as shown by four A/I ratios ranging between 0.421 and 0.384, and assigned to aminozone E1 (Table 1; Hearty and Kaufman, 2009). The age of the underlying Unit C is unclear. The A/I ratio obtained from this unit correlates with aminozone F, suggesting a MIS 7 age (Table 1; Hearty and Kaufman, 2009). However, the important micritization observed in the measured sample indicates this value could have been affected by pedogenic processes. Alternatively, it could be matched with the reversing trend in A/I values identified by Hearty (2010). We conclude that Unit 5 likely dates from the middle or the early part of the Pleistocene.

Comparison with previous work

Building on a glacio-eustatic model originally based on observations from Bermuda (Bretz, 1960; Land et al., 1967), Wanless and Dravis (1989, 2008) correlated the deposition of shallowing-upward sequence with episodes of sea-level highstand during distinct interglacial periods, and the formation of calcrete/soil zones with times of exposure correlated with glaciations. They only identified two reef to oolite sequences in the upper 9.5 m of core # 12, and interpreted each to have formed during one single sea-level highstand. They suggested, however, that at Boat Cove, the sequences may have formed "during different phases of the Sangamon interglacial highstand" (i.e. MIS 5e). In this paper, we show that the upper 7.8 m of core # 12 at Boat Cove contain two (not just one) reef to oolite sequences (Units 1 and 2), separated by a discrete pedogenic zone, both dating from the last interglacial period. The underlying reef to oolite sequence (Units 3+4, between 7.8 and 9.5 m) must not be correlated with the penultimate (MIS 7) or the previous interglacial (MIS 9), but with an older event (MIS 11).

Wanless and Dravis (1989, 2008) associated the two oolitic grainstone sequences from Company Point (Units A and B, core # 4) with the "last two sea-level highstands of the Pleistocene" (i.e. MIS 5e and MIS 7). Our new geochronological results show that these two sequences were formed during two distinctive sea-level events during MIS 5e, and can likely be correlated with the uppermost reef to oolite sequences identified at Boat Cove (Fig. 11). Finally, as mentioned above, the basal Unit C dates from the middle or the early Pleistocene, but probably not from the Pliocene (Wanless and Dravis, 1989) because aragonitic bioclasts are still preserved in this lithology.

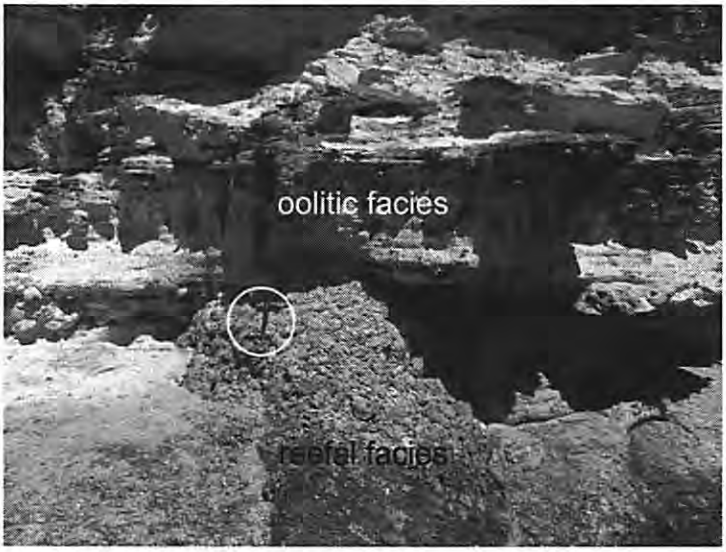

Figure 10. Field example of upper Pleistocene reef to oolite sequence observed near Boat Cove. This sequence likely corresponds to Unit 1 in core # 12. Hammer (in white circle) for scale is 36 cm long.

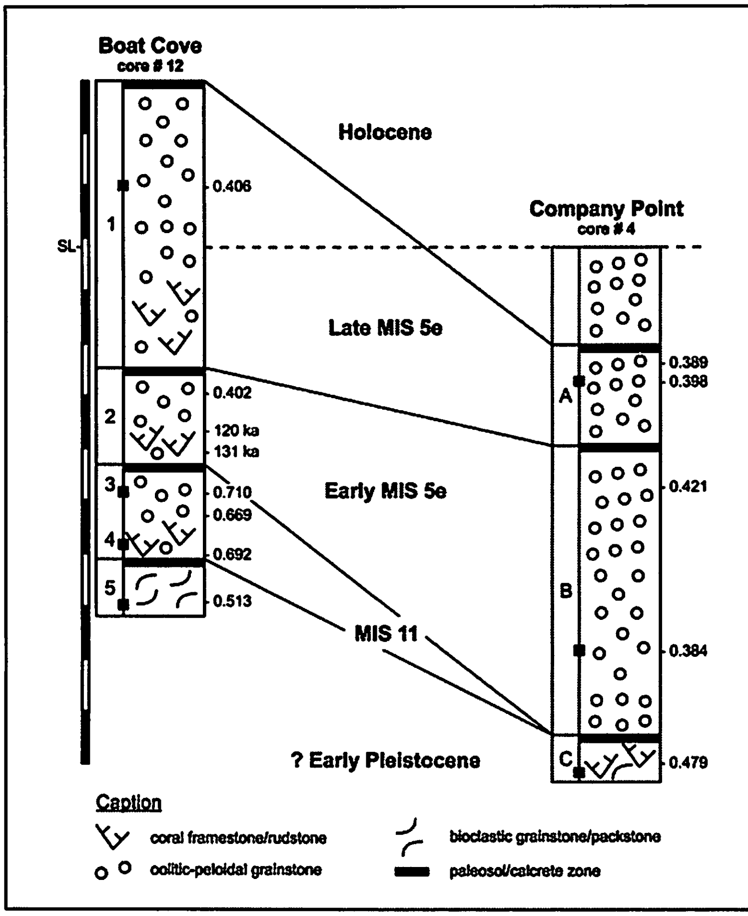

Figure 11. Correlation between the two studied cores. Black and white rectangles in vertical scale bar each correspond to 1 m; black squares show the position of photographed samples (Figures 3 to 6, in descending order, for core # 12, and Figures 7 to 9 for core # 4). A/I ratios and U-Th ages (in ka) are given on the right side of the lithological logs. SL = sea level.

CONCLUSIONS

Our revision of two of the West Caicos cores brings some refinements to the stratigraphy of this island that will need consideration when revising the evolution of the leeward margin of the Caicos platform during the Pleistocene. In addition, our new results demonstrate the limits of the "glacio-eustatic model" often used to decipher the stratigraphy of carbonate islands in the northwestern Atlantic Ocean (Bretz, 1960; Garrett and Gould, 1984). As shown by our data from Boat Cove and Company Point, several shallowing-upward sequences separated by soil zones formed during the last interglacial (MIS 5e), implying a complex sea-level history during this time period (Hearty et al., 2007; Blanchon et al., 2009). However, the precise details of sea-level fluctuations during MIS 5e (i.e. two highstands separated by a lowstand, or one single but complex highstand) cannot be deciphered from our core record.

Conversely, as observed in the Boat Cove core, two vertically stacked shallowing-upward sequences may be separated by a paleosol comprising several glacial/interglacial cycles and may result, for example, in the superposition of MIS 11 and MIS 5e rock units. Such a succession is not uncommon in the Bahamas region (Hearty, 1998) and suggests that sea-level stands during MIS 9 and MIS 7 were too low to allow for the accumulation of significant deposits on the platform top. Last, but not least, our work shows that the lateral correlation of meter-scale shallowing-upward sedimentary successions, i.e. parasequences, is not always straightforward.

ACKNOWLEDGMENTS

We are very grateful to H.R. Wanless and J.J. Dravis for introducing us to the geology of West Caicos and for allowing us to study and resample their cores. We thank F. Gischig and P. Desjacques (University of Geneva) for thin-section manufacturing, D. Kaufman and J. Bright (Northern Arizona University) for providing us the amino-acid racemization data, and A. Eisenhauer (IFM-GEOMAR, Kiel) for U-Th analyses. PK's travel expenses were supported by the Swiss National Science Foundation (grants n° 200020-113356 and n° 200020-124608/1).We also thank H.A. Curran and J.E. Mylroie for constructive reviews of a previous manuscript.

REFERENCES

Blanchon, P., Eisenhauer A., Fietzke J., Liebetrau V., 2009, Rapid sea-level rise and reef back-stepping at the close of the last interglacial highstand, v. 458, p. 881-884.

Bassinot, F.C., Labeyrie, L.D., Vincent, E., Quidelleur, X., Shackleton, N.J., and Lancelot, Y., 1994, The astronomical theory of climate and the age of the Brunhes-Matuyama magnetic reversal: Earth and Planetary Science Letters, v. 126, p. 91-108.

Bretz, JH., 1960, Bermuda: a partially drowned, late mature, Pleistocene karst: Geological Society of America Bulletin, v. 71, p. 1729-1754.

Brown, R.H., 1985, Amino Acid Dating: Origins, v. 12, p. 8-25.

Carew, J.L., and Mylroie J.E., 1995. A stratigraphic and depositional model for the Bahamas Islands, *in* Curran, H.A., and White, B., eds, Terrestrial and Shallow Marine Geology of the Bahamas and Bermuda: Geological Society of America Special Paper, v. 300, p. 5-31.

Caputo, M.V., 1995, Sedimentary architecture of Pleistocene eolian calcarenites, San Salvador Island, Bahamas, *in* Curran, H.A., and White, B., eds, Terrestrial and Shallow Marine Geology of the Bahamas and Bermuda: Geological Society of America Special Paper, v. 300, p. 63-76.

Dravis, J.J., and Wanless, H.R., 2008, Caicos platform models of Quaternary carbonate deposition controlled by stronger easterly trade winds - applications to petroleum exploration, *in* Morgan, W.A., and Harris, P.M., eds, Developing models and analogs for isolated carbonate platforms - Holocene and Pleistocene carbonates of Caicos Platform, British West Indies: SEPM Core Workshop, v. 22, p. 21-27.

Edwards, R.L., Gallup, C.D., and Cheng, H., 2003, Uranium-series dating of marine and lacustrine carbonates, *in* Bourdon, B., Henderson, G.M., Lundstrom, C.C., and Turner, S.P., eds, Uranium-series geochemistry: Reviews in Mineralogy and Geochemistry, v. 52, p. 363-405.

Fietzke, J., Liebetrau, V., Eisenhauer, A., and Dullo, C., 2005, Determination of uranium isotope ratios by multi-static MIC-ICP-MS: method and implementation for precise U- and Th-series isotope measurements: Journal of Analytical Atomic Spectrometry, v. 20, p. 395-401.

Flügel, E., 2004, Microfacies of carbonate rocks: Springer Verlag, Berlin , 976 p.

Fruijtier, C., Elliott, T., and Schlager, W., 2000, Mass-spectrometric ^{234}U-^{230}Th ages from the Key Largo Formation, Florida Keys, United States: constraints on diagenetic age disturbance: Geological Society of America Bulletin, v. 112, p. 267-277.

Garrett, P., and Gould, S.J., 1984, Geology of New Providence Island, Bahamas: Geological Society of America Bulletin, v. 95, p. 209-220.

Hearty, P.J., 1998, The geology of Eleuthera Island, Bahamas: a rosetta stone of Quaternary stratigraphy and sea-level history: Quaternary Science Reviews, v. 17, p. 333-355.

Hearty, P., 2010, Chronostratigraphy and morphological changes in *Cerion* land snail shells over the past 130 ka on Long Island, Bahamas: Quaternary Geochronology, v. 5, p. 50-64.

Hearty, P.J., Hollin J.T., Neumann A.C., O'Leary, M.J., and McCulloch M., 2007, Global sea-level fluctuations during the Last Interglaciation (MIS 5e): Quaternary Science Reviews, v. 26, p. 2090-2112.

Hearty, P.J., and Kaufman D.S., 2000, Whole-rock aminostratigraphy and Quaternary sea-level history of the Bahamas: Quaternary Research, v. 54, p. 163-173.

Hearty, P.J., and Kaufman, D.S., 2009, A *Cerion*-based chronostratigraphy and age model from the Central Bahama Islands: amino-acid racemization and ^{14}C in land snails and sediments: Quaternary Geochronology, v. 4, p. 148-159.

Hearty, P.J., Vacher, H.L., and Mitterer, R.M., 1992, Aminostratigraphy and ages of Pleistocene limestones of Bermuda: Geological Society of America Bulletin, v. 104, p. 471-480.

Hillgärtner, H., Dupraz, C., and Hug, W., 2001, Microbially induced cementation of carbonate sands: are micritic meniscus cements good indicators of vadose diagenesis ?: Sedimentology, v. 48, p. 117-131.

James, N.J., 1974, Diagenesis of scleratinian coral in the subaerial vadose environment: Journal of Paleontology, v. 48, p. 785-799.

Kindler, P., Mylroie J.E., Curran, H.A., Carew, J.L., Gamble, D.W., Rothfus, T.A., Savarese, M., and Sealey, N.E., 2010, Geology of Central Eleuthera, Bahamas: A Field Trip Guide: San Salvador, Bahamas, Gerace Research Centre, 74 p.

Kindler, P., Reyss, J.-L., Cazala, C., and Plagnes, V., 2007, Discovery of a composite reefal terrace of middle and late Pleistocene age in Great Inagua Island, Bahamas. Implications for regional tectonics and sea-level history: Sedimentary Geology, v. 194, p. 141-147.

Land, L.S., MacKenzie, F.T., and Gould, S.J., 1967, Pleistocene history of Bermuda: Geological Society of America Bulletin, v. 78, p. 993-1006.

Lloyd, R.M., Perkins R.D., and Kerr S.D., 1987, Beach and shoreface ooid deposition on shallow interior banks, Turks and Caicos Islands, British West Indies: Journal of Sedimentary Petrology, v. 57, p. 976-982.

Mitterer, R.M., 1968. Amino-acid composition of organic matrix in calcareous oolites: Science, v. 162, p. 1498-1499.

Rankey, E.C., Reeder, S.L., and Correa, T.B.S, 2008, Geomorphology and sedimentology of Ambergris ooid shoal, Caicos Platform, *in* Morgan, W.A., and Harris, P.M., eds, Developing models and analogs for isolated carbonate platforms - Holocene and Pleistocene carbonates of Caicos Platform, British West Indies: SEPM Core Workshop, v. 22, p. 127-132.

Siddall, M., Hönisch, B., Waelbroeck, C., and Huybers, P., 2010, Changes in deep Pacific temperature during the mid-Pleistocene transition and Quaternary: Quaternary Science Reviews, v. 29, p. 170-181.

Thompson, W.G., and Goldstein, S.L., 2005, Open-system coral ages reveal persistent suborbital sea-level cycles: Science, v. 308, p. 401-404.

Waltz, M.D., 1988, The evolution of shallowing-upwards reef to oolite sequences at the leeward margin of Caicos Platform: Unpublished M.S. Thesis, University of Miami, Coral Gables, 95 p.

Wanless, H.R., and Dravis J.J., 1989, Carbonate environments and sequences of Caicos Platform: 28th International Geological Congress Guidebook T374, 75 p.

Wanless, H.R., and Dravis, J.J., 2008. Pleistocene reefal and oolitic core sequences from West Caicos, Caicos, *in* Morgan, W.A., and Harris, P.M., eds, Developing models and analogs for isolated carbonate platforms - Holocene and Pleistocene carbonates of Caicos Platform, British West Indies: SEPM Core Workshop, v. 22, p. 171-175.